

**Dissipation-sensitive multiphoton excitations of strongly interacting Rydberg atoms**

Jing Qian\* and Weiping Zhang

*Quantum Institute for Light and Atoms, Department of Physics, East China Normal University, Shanghai 200062, People's Republic of China*

(Received 20 June 2014; published 8 September 2014)

We theoretically investigate the effect of dissipation on multiphoton excitation of Rydberg atoms. The steady states and the dynamics are compared via two types of four-level excitation schemes with different dissipative paths of spontaneous emission. We find that in the case of strong Rydberg-Rydberg interaction, the schemes will settle in several different nonequilibrium steady states. The interesting aspect is that there exist the multistable steady states, which reveals the competition between interaction-induced nonlinearity and dissipation caused by spontaneous emission. A numerical simulation on the Rydberg population dynamics in the bistable region exhibits different features existing in the two schemes even with the same initial conditions, which accounts for the influence of the dissipation on the dynamics.

DOI: [10.1103/PhysRevA.90.033406](https://doi.org/10.1103/PhysRevA.90.033406)

PACS number(s): 32.80.Rm, 32.80.Ee, 05.70.Ln

**I. INTRODUCTION**

Due to the large electric dipole moments, there are strong and long-range interactions between Rydberg atoms, and these interactions can be controlled and enhanced by external electromagnetic fields. Besides, the huge polarizability of Rydberg states gives rise to giant Kerr coefficients [1], allowing nonlinear optical effects for only a few photons [2]. That is why the atoms excited to the high-lying Rydberg states are of great interest in the recent researches of quantum many-body physics [3], quantum information processing [4], and quantum nonlinear optics [2].

The high-lying Rydberg states can be a bit more easily excited from atomic ground states by laser light via absorption of more than one photon [5], while the spontaneous emission of the intermediary states will introduce the dissipative mechanism into the Rydberg excitation schemes in spite of the long life of the Rydberg states [6]. In general, these environment-induced dissipations inevitably lead to decoherence and noise in the quantum system and thus are undesirable in the above quantum physics researches.

In recent years, however, the dissipation has been altered its role into a useful resource and tool for a lot of quantum applications, such as dissipative state engineering in trapped ions [7,8] and cold atoms [9], dissipative quantum computation [10], dissipative quantum optics [11], bound state formation in molecules [12], and entangled steady-state production [13–15]. The key for these applications is the occurrence of “nonequilibrium stationary state,” which can be achieved when the driving and dissipative processes arrive at a dynamical equilibrium [16–19]. By appropriately arranging the system-environment couplings, these steady states can deviate far from the classical thermal equilibrium states and keep unique quantum features resisting decoherences [20]. Moreover, combining with the strong dipole-dipole interaction and blockade mechanics of the Rydberg atoms, the dissipation could give rise to quite a few exotic phases of ultracold many-body atomic system, such as uniform phase, antiferromagnetic phase, oscillatory phase, and even the bistability between these phases [21–23].

In this work we investigate the effect of dissipation on the steady states and dynamics of multiphoton Rydberg excitation

schemes. To focus on the dissipation induced by the spontaneous emission of the intermediary states, we choose two typical four-level schemes: one level structure is  $N$ -type and the other is cascade. By appropriately arranging the laser fields, these two schemes have exactly the same coherent dynamics. However, if including the effect of dissipation their realistic dynamics are of great difference, since a dissipative channel due to spontaneous decay running in the opposite direction in the two schemes. We compare their nonequilibrium steady states by solving the stationary master equations under the mean-field treatment and find that the number and distribution of their steady-state solutions are entirely different when the Rydberg nonlinear interaction is strong. The bistable steady states are present in the the  $N$ -type scheme while the Autler-Townes splitting (ATS) occurs in the cascade scheme resulting in the tristable steady states. As a consequence, for a strong nonlinear system such as Rydberg atom systems, dissipative force should be considered very carefully since the final steady states of the system will be very sensitive to it. Furthermore, we study the dynamical evolution of the two schemes in the bistable region. Due to the difference in the dissipative channel, we observe two schemes may evolve into different branches under the same initial conditions, which makes sense for dissipative preparation of quantum state in strong nonlinear interacting systems.

**II. MODEL AND MASTER EQUATION**

In what follows, we discuss two different multistep cw-excitation schemes for the Rydberg state, as typically used in experiments. One is an  $N$ -type scheme with a Raman transition before a Rydberg-excited transition, as shown in Fig. 1(a). The atom is first excited from its ground state  $|g\rangle$  to an intermediate state  $|e\rangle$  with a transition strength given by the Rabi frequency  $\Omega_g$  and then transits to a metastable state  $|s\rangle$  with Rabi frequency  $\Omega_s$ . Finally, another laser drives the transition between the metastable level and the desired Rydberg state  $|r\rangle$  with Rabi frequency  $\Omega_r$ . The photon for the Raman transition is typically provided by the Magneto-Optical trap lasers, which are tuned on resonance with the levels during the time of Rydberg excitation. So the spontaneous emissions from the intermediate state  $|e\rangle$  to state  $|g\rangle$  with rate  $\Gamma$  and to state  $|s\rangle$  with rate  $\gamma$ , respectively, have to be taken into account. On the other hand, we allow for a detuning  $\Delta$  from

\*Corresponding author: [jqian1982@gmail.com](mailto:jqian1982@gmail.com)

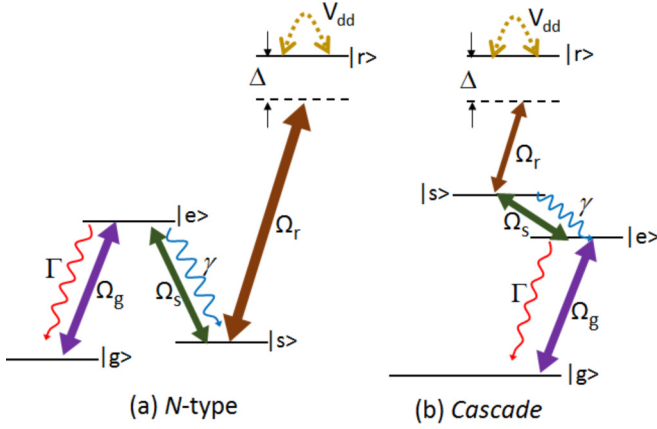


FIG. 1. (Color online)  $N$ -type and cascade atomic multilevel systems. States  $|g\rangle$ ,  $|e\rangle$ ,  $|s\rangle$ , and  $|r\rangle$  respectively show the ground state, two intermediate states, and Rydberg state, which are successively coupled by laser Rabi frequencies  $\Omega_g$ ,  $\Omega_s$ , and  $\Omega_r$ . The three-photon laser detuning  $\Delta$  can be controlled in experiment. Other parameters are described in the text.

resonant Rydberg excitation and the lifetime of the Rydberg state is much longer (typically as large as tens of  $\mu\text{s}$  with the principle quantum number  $n \sim 50$ ) so that its decay can be safely neglected in our discussion. The second scheme shown in Fig. 1(b) has a cascade level structure, where  $|s\rangle$  represents the higher intermediate state, so that  $\gamma$  is the decay rate from state  $|s\rangle$  to state  $|e\rangle$ , opposite to the case in the first scheme. The physical meanings of the other quantities remain unchanged. Besides, we note that in this scheme decay from state  $|s\rangle$  to state  $|g\rangle$  is physically forbidden according to the transition selection rule. Except the atom-light interaction, we also consider the strong interaction between Rydberg atoms (here we only consider a homogeneous van der Waals interaction), which under the mean-field approximation will cause a population-dependent energy shift to the Rydberg state.

Mean-field theory is a classical approximation to the quantum model in which quantum correlations between atoms are ignored. Note that it works well only with large atom number [24]. For systems of several Rydberg atoms, the quantum effect of the strong Rydberg blockade can no longer be effectively described by the mean-field approximation [25–28]. In our consideration, we assume that the number of atom is large enough so that the mean-field approach can be safely used.

In frames rotating at appropriate frequencies respectively, these two different Rydberg-excitation schemes can be described by a same mean-field Hamiltonian ( $\hbar = 1$ ),

$$\mathcal{H} = (\Delta + V_{dd}\rho_{rr})\sigma_{rr} + (\Omega_g\sigma_{ge} + \Omega_s\sigma_{es} + \Omega_r\sigma_{sr} + \text{H.c.}), \quad (1)$$

with  $\sigma_{ij} = |i\rangle\langle j|$  being the corresponding transition operator between two internal atomic states,  $V_{dd}$  the Rydberg interaction strength, and  $\rho_{rr}$  the Rydberg state population. The only difference is the expression of the three-photon detuning, given by  $\Delta = \omega_r - \omega_{\Omega_g} \mp \omega_{\Omega_s} - \omega_{\Omega_r}$  with frequencies  $\omega_r$ ,  $\omega_{\Omega_g}$ ,  $\omega_{\Omega_s}$ , and  $\omega_{\Omega_r}$  denoting the energy of state  $|r\rangle$  and the carrier frequencies of the fields  $\Omega_g$ ,  $\Omega_s$ , and  $\Omega_r$ , respectively. The upper sign is for the  $N$ -type scheme and the lower one is for the cascade scheme. That means the coherent dynamics

of these two schemes can be same even though they have different structures of energy levels, provided the three-photon detunings are equal. However, we show below that in a realistic experiment where the dissipation caused by the spontaneous decay should be considered, these schemes will display distinct nonequilibrium steady states and dynamics, which are attributed to the opposite direction of decay route between level  $|s\rangle$  and level  $|e\rangle$  in two schemes.

In order to investigate the influences of the spontaneous emissions from the intermediate excited states, we use the Lindblad master equation [29]

$$\partial_t \hat{\rho} = -i[\mathcal{H}, \hat{\rho}] + \mathcal{L}[\hat{\rho}], \quad (2)$$

where  $\hat{\rho}$  is the single-atom density matrix operator which can well capture the evolution of the Rydberg atoms according to the mean-field approximation, and  $\mathcal{L}[\hat{\rho}]$  is the Lindblad operator which is introduced phenomenologically to depict the atomic spontaneous emissions due to optical excitations [30]:

$$\mathcal{L}[\hat{\rho}] = \frac{\Gamma}{2}(2\sigma_{ge}\hat{\rho}\sigma_{ge}^\dagger - \{\sigma_{ee}, \hat{\rho}\}) + \frac{\gamma}{2}(2\hat{\rho}d^\dagger - \{d^\dagger d, \hat{\rho}\}), \quad (3)$$

where  $\{A, B\} = AB + BA$ , and  $d = \sigma_{se}$  for the  $N$ -type system and  $\sigma_{es}$  for the cascade system. From that we can obtain two different groups of differential equations of the density matrix elements  $\rho_{ij}$ . For the  $N$ -type system we have

$$\begin{aligned} \dot{\rho}_{ee} &= 2\Omega_g \text{Im}(\rho_{ge}) - 2\Omega_s \text{Im}(\rho_{es}) - (\gamma + 1)\rho_{ee}, \\ \dot{\rho}_{ss} &= 2\Omega_s \text{Im}(\rho_{es}) - 2\Omega_r \text{Im}(\rho_{sr}) + \gamma\rho_{ee}, \\ \dot{\rho}_{rr} &= 2\Omega_r \text{Im}(\rho_{sr}), \\ \dot{\rho}_{ge} &= -i\Omega_g(\rho_{ee} - \rho_{gg}) + i\Omega_s\rho_{gs} - \frac{\gamma + 1}{2}\rho_{ge}, \\ \dot{\rho}_{gs} &= -i\Omega_g\rho_{es} + i\Omega_s\rho_{ge} + i\Omega_r\rho_{gr}, \\ \dot{\rho}_{gr} &= i\Delta_{\text{eff}}\rho_{gr} - i\Omega_g\rho_{er} + i\Omega_r\rho_{gs}, \\ \dot{\rho}_{es} &= -i\Omega_g\rho_{gs} - i\Omega_s(\rho_{ss} - \rho_{ee}) + i\Omega_r\rho_{er} - \frac{\gamma + 1}{2}\rho_{es}, \\ \dot{\rho}_{er} &= \left(i\Delta_{\text{eff}} - \frac{\gamma + 1}{2}\right)\rho_{er} - i\Omega_g\rho_{gr} - i\Omega_s\rho_{sr} + i\Omega_r\rho_{es}, \\ \dot{\rho}_{sr} &= i\Delta_{\text{eff}}\rho_{sr} - i\Omega_s\rho_{er} - i\Omega_r(\rho_{rr} - \rho_{ss}), \end{aligned} \quad (4)$$

while for the cascade system

$$\begin{aligned} \dot{\rho}_{ee} &= 2\Omega_g \text{Im}(\rho_{ge}) - 2\Omega_s \text{Im}(\rho_{es}) - \rho_{ee} + \gamma\rho_{ss}, \\ \dot{\rho}_{ss} &= 2\Omega_s \text{Im}(\rho_{es}) - 2\Omega_r \text{Im}(\rho_{sr}) - \gamma\rho_{ss}, \\ \dot{\rho}_{rr} &= 2\Omega_r \text{Im}(\rho_{sr}) \\ \dot{\rho}_{ge} &= -i\Omega_g(\rho_{ee} - \rho_{gg}) + i\Omega_s\rho_{gs} - \frac{1}{2}\rho_{ge}, \\ \dot{\rho}_{gs} &= -i\Omega_g\rho_{es} + i\Omega_s\rho_{ge} + i\Omega_r\rho_{gr} - \frac{\gamma}{2}\rho_{gs}, \\ \dot{\rho}_{gr} &= i\Delta_{\text{eff}}\rho_{gr} - i\Omega_g\rho_{er} + i\Omega_r\rho_{gs}, \\ \dot{\rho}_{es} &= -i\Omega_g\rho_{gs} - i\Omega_s(\rho_{ss} - \rho_{ee}) + i\Omega_r\rho_{er} - \frac{\gamma + 1}{2}\rho_{es}, \\ \dot{\rho}_{er} &= \left(i\Delta_{\text{eff}} - \frac{1}{2}\right)\rho_{er} - i\Omega_g\rho_{gr} - i\Omega_s\rho_{sr} + i\Omega_r\rho_{es}, \\ \dot{\rho}_{sr} &= \left(i\Delta_{\text{eff}} - \frac{\gamma}{2}\right)\rho_{sr} - i\Omega_s\rho_{er} - i\Omega_r(\rho_{rr} - \rho_{ss}), \end{aligned} \quad (5)$$

where we have assumed that the off-diagonal coherence elements  $\rho_{ij} = \rho_{ji}^*$  ( $i \neq j$ ) and the conservation of the total population that the diagonal elements  $\rho_{gg} + \rho_{ee} + \rho_{ss} + \rho_{rr} = 1$ . The effective detuning  $\Delta_{\text{eff}} = \Delta + V_{dd}\rho_{rr}$ , including the population-dependent frequency shift of the Rydberg state, which makes the differential equations nonlinear. We can find these two groups of equations become identical when the decay  $\gamma \rightarrow 0$ , which means the dynamics of the two schemes are indistinguishable. Instead, a nonvanishing  $\gamma$  will lead to entirely different excitation dynamics, especially in the regions with high nonlinearity induced by Rydberg-Rydberg interaction. To show these differences in the following we keep the common decay  $\Gamma$  constant and focus on the influence of the decay  $\gamma$  which has opposite direction in the two schemes. Then it is also convenient to renormalize the time by  $\Gamma^{-1}$  and all frequencies by  $\Gamma$  in the equations.

### III. STEADY STATES AND PHASE DIAGRAM

We first investigate the steady states of the schemes, where the competition between the oscillation caused by coherent optical driving and the dissipation due to the spontaneous emissions reaches a dynamical equilibrium so that the populations and the coherence for each level become stationary. The steady occupancy of the Rydberg state,  $\rho_{rr}$ , can then be readily obtained by setting all time differential terms in Eqs. (4) and (5) equal to zero and then solving the resulting algebraic equations. For the  $N$ -type scheme, we obtain a cubic equation about  $\rho_{rr}$ , which may have one or three solutions corresponding to the uniform and the bistable phase of the Rydberg excitation scheme, respectively (we should check the stabilities of these solutions to ensure they are achievable in the dissipation environment). Here the bistable phase, as a typical nonlinear effect, is caused by the Rydberg-Rydberg interaction. It has been observed in recent experiment of a dilute Rydberg atomic ensemble [24]. On the other side, the equation becomes quintic in the case of the cascade scheme, indicating the existence of multistable phase of the scheme, which has not been found in the Rydberg system. The analytical forms of these equations and their solutions are too cumbersome to present here, so we instead show the phase diagram of the Rydberg atoms in the parameter space of  $\Omega_r$  and  $\Delta$ , which is decided by the number of the stable solutions. As shown in Fig. 2, the left column is for the  $N$ -type scheme and the right column for the cascade scheme, with the regions labeled by numbers 0–3 respectively corresponding to the oscillatory phase (no stable solution), the uniform phase (only one stable solution), bistable phase (two stable solutions), and tristable phase (three stable solutions).

From the figure we can find the two schemes have similar phase diagrams at small decay strength (see the first row,  $\gamma = 0.01\Gamma$  and  $V_{dd} = -50\Gamma$ ). The parameter space is dominated by the uniform phase, the bistable phase presents for small Rabi frequency  $\Omega_r$ , and the oscillatory phase only survives in a very narrow region where detuning  $\Delta$  is small. For a large value of  $\gamma$  (the second row,  $\gamma = \Gamma$  and  $V_{dd} = -50\Gamma$ ), the phase diagrams become distinct from each other. In the case of the  $N$ -type scheme the oscillatory phase occupies a large area with larger values of  $\Omega_r$ , which is because the nonlossy states,  $|s\rangle$  and  $|r\rangle$ , sustain a Rabi-type population oscillation between them. Instead, in the case of the cascade scheme the

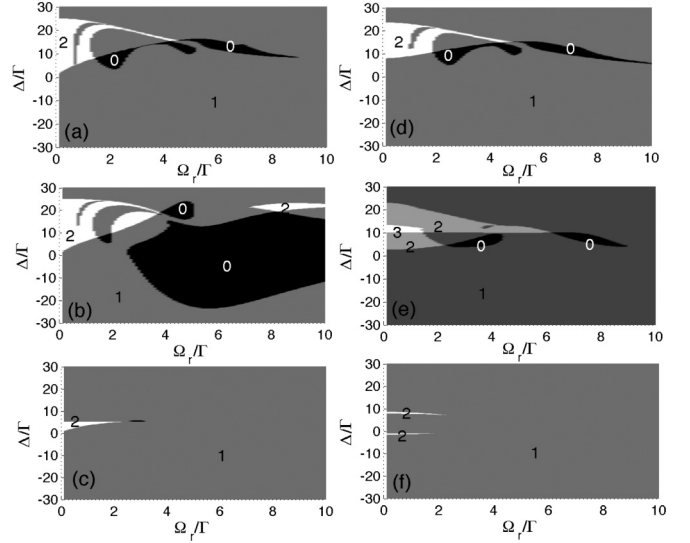


FIG. 2. Phase diagram in the  $(\Omega_r, \Delta)$  space, indicating the influence of decay and nonlinearity on the phase of the Rydberg atoms, with the numbers of the stable solutions marked in different gray shades. The left column is for the  $N$ -type system and the right column is for the cascade one. From top to bottom, we fix the Rabi frequencies  $\Omega_g = 5.0$ ,  $\Omega_s = 2.0$ , and change the strength of decay and Rydberg interaction: (a) and (d)  $V_{dd} = -50$  and  $\gamma = 0.01$ ; (b) and (e)  $V_{dd} = -50$  and  $\gamma = 1.0$ ; (c) and (f)  $V_{dd} = -10$  and  $\gamma = 1.0$ . (All parameters are scaled by  $\Gamma$ .)

decay of state  $|s\rangle$  prevents such oscillation. Moreover, ATS of the cascade system causes a unique tristable phase (we show it clearly below) which is absent in the former case [31]. We emphasize that the effect of dissipation-sensitive steady states is more remarkable under the condition of strong nonlinearity. When we decrease the Rydberg-Rydberg interaction strength, the phase diagrams of the two schemes trends to be analogous even for large values of decay (the third row,  $\gamma = \Gamma$  and  $V_{dd} = -10\Gamma$ ).

Before focusing on the different quantum multistable phases of the two schemes in the parameter space of strong nonlinearity and large decay, we first investigate their steady states without nonlinearity, which will show the cause of these differences are the direction of the decay  $\gamma$ . By solving the stationary Optical Bloch equations (OBEs) in the case of  $V_{dd} = 0$  and keeping the other parameters the same as in Figs. 2(b) and 2(e), we observe that the Rydberg excitation spectrum in the cascade scheme shows a double-peak structure separated by  $2\Omega_g$  which is same as the feature of the ATS presenting in the three-level Rydberg-excitation scheme [32,33]. In our cascade scheme, the same direction of decay  $\gamma$  and  $\Gamma$  makes the atoms populate mostly on states  $|e\rangle$  and  $|g\rangle$ , resulting in the splitting of the Rydberg excitation spectrum. Moreover, unlike in the three-level scheme where ATS is just an effect of transient stability [34], the existence of the intermediate state  $|s\rangle$  here has stabilized this splitting and enabled it to appear in the final steady state of the scheme. In the case of the  $N$ -type scheme, the opposite directions of decays  $\gamma$  and  $\Gamma$ , as well as small Rabi frequency  $\Omega_s$ , may accumulate the population on state  $|s\rangle$  only, giving rise to a single peak instead of the ATS in the Rydberg excitation spectrum. These different peak structures

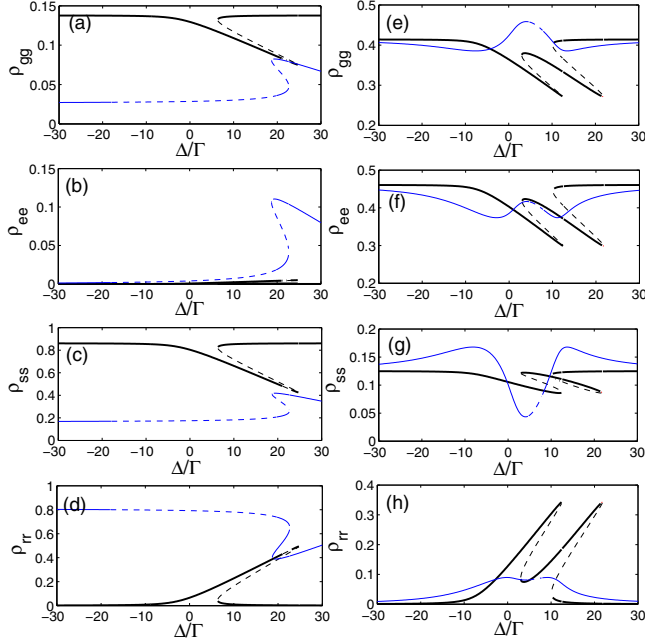


FIG. 3. (Color online) The steady-state populations of state  $|g\rangle$  (first row), state  $|e\rangle$  (second row), state  $|s\rangle$  (third row), and  $|r\rangle$  (last row) are plotted as a function of three-photon detuning  $\Delta$ , with the weak Rydberg-state coupling case ( $\Omega_r/\Gamma = 1.0$ ) in thick black curves and the strong coupling case ( $\Omega_r/\Gamma = 8.0$ ) in thin blue (gray) curves. The dashed curves correspond to the values in the unstable phases. The left and right columns are for the  $N$ -type system and the cascade system, respectively. Other parameters are same as Figs. 2(b) and 2(e).

still remain in the presence of Rydberg-Rydberg interactions. As we show in Figs. 3(a)–3(h), the nonlinearity caused by the interaction distorts the original spectrum, resulting in the different multistable steady states of the cascade and the  $N$ -type schemes.

Again the left column of Fig. 3 is for the  $N$ -type scheme, where we display the exact values of the steady population of each states at small  $\Omega_r$  case (thick black line) and large  $\Omega_r$  case (thin blue [gray] line), respectively, corresponding to the two bistable regions marked in phase diagram Fig. 2(b). We can find different features of the bistable behaviors in these two cases. When  $\Omega_r$  is small it exhibits intrinsic bistability in the region of  $\Delta_{\text{eff}} = \Delta + V_{dd}\rho_{rr} \approx 0$  with its inclined direction of hysteresis window depending on the sign of Rydberg interaction  $V_{dd}$ . When  $\Delta$  is negative or large positive (i.e.,  $\Delta_{\text{eff}}$  is off-resonance), the ground state  $|s\rangle$  is occupied with a dominant number of atoms ( $\rho_{ss} > 0.8$ ). However, as increasing  $\Omega_r$  to 8.0 we find that the dominant population at  $|\Delta| \rightarrow \infty$  occupies the Rydberg state  $|r\rangle$  with its value  $\rho_{rr} \rightarrow \Omega_g^2 \Omega_r^4 / [(\Omega_g^2 + \Omega_s^2)^3 + \Omega_g^2 \Omega_r^4]$  due to a quite strong Rydberg excitation. Meanwhile, a small region of bistable phase emerges near  $\Delta/\Gamma = 20$  where the Rydberg-interaction-induced energy shift has been compensated by a large detuning, i.e.,  $\Delta_{\text{eff}} \approx 0$ . Besides, when  $\Omega_r$  is large, there is a large unstable region (corresponding to the oscillatory phase) denoted by the dashed lines, which is due to the strong coupling between the nonlossy states  $|s\rangle$  and  $|r\rangle$ .

Turning to the case of the cascade system (the right column of Fig. 3), a dramatic difference is the presence of the inclined double-peak configuration at small  $\Omega_r$  case, which gives rise to bistable and even tristable phases when  $\Delta$  and  $|V_{dd}| \rho_{rr}$  are comparable. In addition, state  $|g\rangle$  and state  $|e\rangle$  share the most atomic population ( $\rho_{gg} + \rho_{ee} > 0.85$ ) and the case does not change much even for larger value of  $\Omega_r$ . However, the double-peak structure degenerates a lot so that there is no multistable phase in large  $\Omega_r$  case. This is due to the comparable values of  $\Omega_g$  and  $\Omega_r$  preventing the occurrence of the ATS.

In summary, for the  $N$ -type scheme, decay  $\gamma$  leads to a large population on state  $|s\rangle$  which, combined with Rydberg state  $|r\rangle$ , makes the scheme work like a two-level system, so that the sustained Rabi-typed oscillation occurs with an intensive  $\Omega_r$ . For small  $\Omega_r$  the behavior of the scheme is closer to the cooperative optical excitation [35]. For the cascade scheme, the existence of  $\gamma$  leads to the ATS phenomenon, inducing multistable steady-state phases under the condition of strong nonlinear interaction.

#### IV. BISTABILITY AND POPULATION DYNAMICS

The above phase diagrams reveal the properties of the steady states in the parameter space of detuning  $\Delta$  and Rabi frequency  $\Omega_r$ , which are controlled by the external lasers. The strong nonlinear interactions that the bistable phases present suggest there are two different steady states, i.e., the low- and the high-Rydberg-occupied steady states, under the same laser parameters. In reality, the system would eventually evolve into one of them, which depends on the initial states and decay routes. In order to study this dependence, we perform a numerical simulation for the population dynamics by directly solving the OBEs (4) and (5).

In the calculation, we choose  $\Omega_r = 1.0$ ,  $\Delta = 15$ , with the other parameters the same as in Figs. 2(b) and 2(e), where the bistable steady state gives two stationary Rydberg populations  $\rho_{rr}^{t \rightarrow \infty} = 0.0047$  (low) and 0.3190 (high) for the  $N$ -type scheme and  $\rho_{rr}^{t \rightarrow \infty} = 0.0047$  (low) and 0.228 (high) for the cascade scheme, respectively. Since the Rydberg state  $|r\rangle$  is not subjected to the dissipation in our model, we fix its initial population by  $\rho_{rr}^{t=0} = 0.19$  for the  $N$ -type scheme and  $\rho_{rr}^{t=0} = 0.16$  for the cascade scheme, and then focus on the dependence of its final population on the initial population of state  $|g\rangle$  and  $|s\rangle$  as depicted in Figs. 4(a) and 4(b). Note that the total particle is always conserved,  $\rho_{gg} + \rho_{ee} + \rho_{ss} + \rho_{rr} = 1$ .

From Fig. 4 we can find difference between the two schemes in the side of small  $\rho_{ss}^{t=0}$ , which means state  $|e\rangle$  and state  $|g\rangle$  are largely occupied at the initial time. For the cascade system whose  $\gamma$  is large and  $\rho_{ss}^{t=0}$  is small, it is hard to pump atoms into the highly excited state  $|r\rangle$ . However, in the  $N$ -type system dissipations from  $|e\rangle$  may create strong atomic correlations among  $|g\rangle$ ,  $|e\rangle$ , and  $|s\rangle$  (e.g., a Raman scattering process [36]), giving rise to an enhancement for population in state  $|s\rangle$ . It is therefore possible to realize a high Rydberg excitation. The final populations  $\rho_{jj}^{t \rightarrow \infty} = (0.0974, 0.0032, 0.5804, 0.3190)$  for the  $N$ -type scheme and  $\rho_{jj}^{t \rightarrow \infty} = (0.4127, 0.4589, 0.1237, 0.0047)$  for the cascade scheme.

On the other side when  $\rho_{ss}^{t=0}$  is large, since state  $|s\rangle$  is directly coupled with state  $|r\rangle$  by laser  $\Omega_r$ , the Rydberg

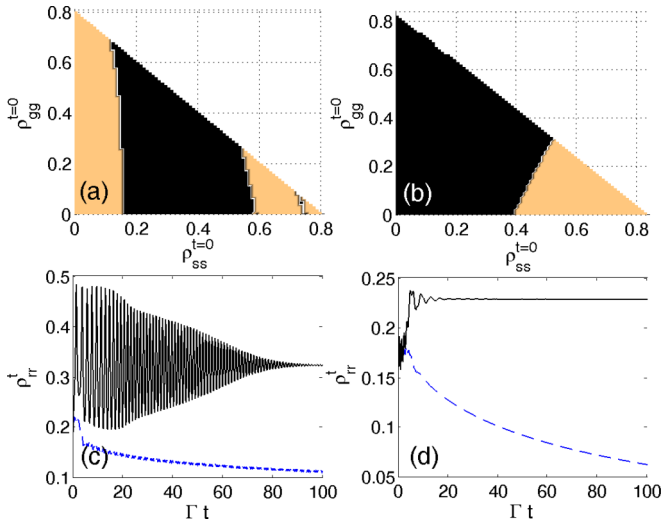


FIG. 4. (Color online) The final Rydberg state population ( $\rho_{rr}^{t \rightarrow \infty}$ ) for (a) the  $N$ -type system and (b) the cascade system, as a function of initial population on the  $s$  state ( $\rho_{ss}^{t=0}$ ) and  $g$  state ( $\rho_{gg}^{t=0}$ ). Dark and light colors represent the low and high Rydberg-state occupancy, respectively. The colorless regions are unstable and without stationary solutions. Panels (c) and (d) show population evolution in the bistable region for the  $N$ -type system and the cascade system, respectively, where  $\rho_{gg}^{t=0} = 0.1$  and  $\rho_{ss}^{t=0} = 0.4$  (dashed blue [gray] line) and 0.7 (solid black line). See the text for other parameters.

excitation is easy. The final populations  $\rho_{jj}^{t \rightarrow \infty} = (0.0974, 0.0032, 0.5804, 0.3190)$  for the  $N$ -type scheme, where the populations in  $|s\rangle$  and  $|r\rangle$  are dominant. For the cascade scheme, due to the effect of decay  $\gamma$  and  $\Gamma$  the situation is different. We have  $\rho_{jj}^{t \rightarrow \infty} = (0.3161, 0.3506, 0.1053, 0.228)$ , where the populations of state  $|g\rangle$  and  $|e\rangle$  are not small.

Except for the above two sides, in the middle region, both of the schemes tend to a low Rydberg occupancy with  $\rho_{jj}^{t \rightarrow \infty} = (0.1373, 0, 0.858, 0.0047)$  for the  $N$ -type scheme, corresponding to a dominant final occupancy of state  $|s\rangle$ , and with  $\rho_{jj}^{t \rightarrow \infty} = (0.4127, 0.4589, 0.1237, 0.0047)$  for the cascade scheme, indicating a population sharing between states  $|g\rangle$  and  $|e\rangle$ .

Finally, we emphasize that even though the final values of the Rydberg population are close, the dynamical evolution process and therefore the time spent on achieving the final stationary states are much different for the two schemes. In Figs. 4(c) and 4(d), we show their different population dynamics for the Rydberg state in the bistable region under the same experimental parameters. In contrast to the case of the cascade scheme, the  $N$ -type scheme is subjected to a strong population oscillation while tending towards the high branch of Rydberg occupancy and it requires more time to reach steady state. This result agrees with our former analysis of bistability

as in Fig. 2(b) that two nonlossy states  $|s\rangle$  and  $|r\rangle$  may lead to unstable oscillations.

## V. EXPERIMENTAL REALIZATION

Before the conclusion, we discuss the experimental realization of our proposed schemes. The three-photon cascade scheme cannot only offer an easier route for the Rydberg excitation but also limit the excited atoms in a narrow velocity distribution, so that it has been adopted in recent experiments to explore the nonequilibrium phase transition in a thermal Rydberg atomic gas [24]. Especially in this experiment, the existence of intrinsic optical bistable effect has been identified as we analyzed in the above theory model. However, according to our theory model we find in this scheme that the tristable phase only exists under quite rigorous parameters as implied in Fig. 2(e), making it a challenge to verify in experiments. As for the  $N$ -type scheme, it is realizable by current experimental technology and has been recently advanced in several theoretical proposals to realize Rydberg quantum simulator [37] and prepare Rydberg-dressed atoms [35].

## VI. CONCLUSION

In an open quantum system where driving and dissipative processes compete with each other and settle the system on a nonequilibrium steady state, a number of novel phenomena absent in the equilibrium system will appear [38]. In this work, we have investigated the effect of dissipation on the steady-state properties and dynamics for the two different excitation schemes of strong interacting Rydberg atoms, one is of the  $N$ -type level structure and the other of the cascade structure. We study the phase diagram of these schemes and find bistable and tristable phases in the region of strong nonlinearity caused by the Rydberg-Rydberg interaction. We investigate the population dynamics of the Rydberg state in bistable region and display its dependence of the initial population distributions. By comparing the steady state and the dynamics of these two schemes, we show their sensitive dependence on the path and the amount of the dissipation caused by the spontaneous emission [39]. Future work will focus on the quantum state preparation [40] and multistable switching [41] in the Rydberg atomic schemes by controlling and arranging the dissipation.

## ACKNOWLEDGMENTS

J.Q. thanks P. Meystre and K. Zhang for useful discussions. This work was supported by the National Basic Research Program of China (973 Program) under Grant No. 2011CB921604, the NSFC under Grants No. 11104076, No. 11474094, and No. 11234003, and the Specialized Research Fund for the Doctoral Program of Higher Education No. 20110076120004.

- [1] A. Mohapatra, M. Bason, B. Butscher, K. Weatherill, and C. Adams, *Nat. Phys.* **4**, 890 (2008).  
 [2] T. Peyronel, O. Firstenberg, Q. Liang, S. Hofferberth, A. Gorshkov, T. Pohl, M. Lukin, and V. Vuletić, *Nature (London)* **488**, 57 (2012).

- [3] See e.g., H. Weimer, Ph.D. dissertation, University of Stuttgart, 2010 (unpublished).  
 [4] M. Saffman, T. Waller, and K. Mølmer, *Rev. Mod. Phys.* **82**, 2313 (2010), and references therein.

- [5] C. Carr, M. Tanasittikosol, A. Sargsyan, D. Sarkisyan, C. Adams, and K. Weatherill, *Opt. Lett.* **37**, 3858 (2012).
- [6] B. Olmos, D. Yu, and I. Lesanovsky, *Phys. Rev. A* **89**, 023616 (2014).
- [7] J. Barreiro, M. Müller, P. Schindler, D. Nigg, T. Monz, M. Chwalla, M. Hennrich, C. Roos, P. Zoller, and R. Blatt, *Nature (London)* **470**, 486 (2011).
- [8] S. Genway, W. Li, C. Ates, B. P. Lanyon, and I. Lesanovsky, *Phys. Rev. Lett.* **112**, 023603 (2014).
- [9] S. Diehl, A. Micheli, A. Kantian, B. Kraus, H. Büchler, and P. Zoller, *Nat. Phys.* **4**, 878 (2008).
- [10] F. Verstraete, M. Wolf, and J. Cirac, *Nat. Phys.* **5**, 633 (2009).
- [11] A. V. Gorshkov, R. Nath, and T. Pohl, *Phys. Rev. Lett.* **110**, 153601 (2013).
- [12] M. Lemesko and H. Weimer, *Nat. Commun.* **4**, 2230 (2013).
- [13] Y. Lin, J. Gaebler, F. Reiter, T. Tan, R. Bowler, A. Sorensen, D. Leibfried, and D. Wineland, *Nature (London)* **504**, 415 (2013).
- [14] D. D. Bhaktavatsala Rao and K. Mølmer, *Phys. Rev. Lett.* **111**, 033606 (2013).
- [15] A. W. Carr and M. Saffman, *Phys. Rev. Lett.* **111**, 033607 (2013).
- [16] S. Diehl, A. Tomadin, A. Micheli, R. Fazio, and P. Zoller, *Phys. Rev. Lett.* **105**, 015702 (2010).
- [17] E. G. Dalla Torre, E. Demler, T. Giamarchi, and E. Altman, *Nat. Phys.* **6**, 806 (2010).
- [18] I. Lesanovsky and J. P. Garrahan, *Phys. Rev. Lett.* **111**, 215305 (2013).
- [19] D. Petrosyan, M. Hönig, and M. Fleischhauer, *Phys. Rev. A* **87**, 053414 (2013).
- [20] I. Lesanovsky and J. P. Garrahan, *Phys. Rev. A* **90**, 011603(R) (2014).
- [21] T. E. Lee, H. Häffner, and M. C. Cross, *Phys. Rev. A* **84**, 031402(R) (2011).
- [22] J. Qian, G. Dong, L. Zhou, and W. Zhang, *Phys. Rev. A* **85**, 065401 (2012).
- [23] A. Hu, T. E. Lee, and C. W. Clarks, *Phys. Rev. A* **88**, 053627 (2013).
- [24] C. Carr, R. Ritter, C. G. Wade, C. S. Adams, and K. J. Weatherill, *Phys. Rev. Lett.* **111**, 113901 (2013).
- [25] E. Urban, T. Johnson, T. Henage, L. Isenhower, D. Yavuz, T. Waller, and M. Saffman, *Nat. Phys.* **5**, 110 (2009).
- [26] A. Gaëtan, Y. Miroshnychenko, T. Wilk, A. Chotia, M. Viteau, D. Comparat, P. Pillet, A. Browaeys, and P. Grangier, *Nat. Phys.* **5**, 115 (2009).
- [27] D. Barredo, S. Ravets, H. Labuhn, L. Béguin, A. Vernier, F. Nogrette, T. Lahaye, and A. Browaeys, *Phys. Rev. Lett.* **112**, 183002 (2014).
- [28] A. M. Hankin, Y. Y. Jau, L. P. Parazzoli, C. W. Chou, D. J. Armstrong, A. J. Landahl, and G. W. Biedermann, *Phys. Rev. A* **89**, 033416 (2014).
- [29] J. Qian, L. Zhou, and W. Zhang, *Phys. Rev. A* **87**, 063421 (2013).
- [30] H. Breuer and F. Petruccione, *The Theory of Open Quantum Systems* (Oxford University Press, Oxford, 2002).
- [31] D. Comparat and P. Pillet, *J. Opt. Soc. Am. B* **27**, A208 (2010).
- [32] C. Ates, T. Pohl, T. Pattard, and J. M. Rost, *Phys. Rev. Lett.* **98**, 023002 (2007).
- [33] T. Amthor, C. Giese, C. S. Hofmann, and M. Weidemüller, *Phys. Rev. Lett.* **104**, 013001 (2010).
- [34] C. Ates, T. Pohl, T. Pattard, and J. M. Rost, *Phys. Rev. A* **76**, 013413 (2007).
- [35] J. Otterbach and M. Lemesko, *Phys. Rev. Lett.* **113**, 070401 (2014).
- [36] C.-H. Yuan, L. Q. Chen, Z. Y. Ou, and W. Zhang, *Phys. Rev. A* **87**, 053835 (2013).
- [37] H. Weimer, M. Müller, I. Lesanovsky, P. Zoller, and H. Büchler, *Nat. Phys.* **6**, 382 (2010).
- [38] A. Tomadin, S. Diehl, and P. Zoller, *Phys. Rev. A* **83**, 013611 (2011).
- [39] A. W. Glaetzle, R. Nath, B. Zhao, G. Pupillo, and P. Zoller, *Phys. Rev. A* **86**, 043403 (2012).
- [40] M. Ebert, A. Gill, M. Gibbons, X. Zhang, M. Saffman, and T. G. Waller, *Phys. Rev. Lett.* **112**, 043602 (2014).
- [41] T. E. Lee, H. Häffner, and M. C. Cross, *Phys. Rev. Lett.* **108**, 023602 (2012).